Theriogenology Wild 5 (2024) 100096

Contents lists available at ScienceDirect

Theriogenology Wild

journal homepage: www.journals.elsevier.com/theriogenology-wild

Follicle-like and other novel structures found in ovaries of aged white rhinoceroses and their potential impact on oocyte recovery rate

R. Appeltant [a,b], R. Hermes [c], S. Holtze [d], T.B. Hildebrandt [d,e], S.A. Williams [a,*]

[a] Nuffield Department of Women's and Reproductive Health, University of Oxford, Women's Centre, Level 3, John Radcliffe Hospital, Oxford, United Kingdom
[b] Gamete Research Centre, Veterinary Physiology and Biochemistry, Department of Veterinary Sciences, University of Antwerp, Wilrijk, Belgium
[c] School of Life and Environmental Sciences, The University of Sydney, Sydney, Australia
[d] Leibniz Institute for Zoo and Wildlife Research, Berlin D-10315, Germany
[e] Freie Universität Berlin, Berlin D-14195, Germany

ARTICLE INFO

Keywords:
Southern white rhinoceros
Histology
Ovary
Follicle
Immunohistochemistry

ABSTRACT

Female rhinoceroses have an ovarian reserve that consists of immature oocytes in primordial follicles. Establishing methods to grow and culture these oocytes from those follicles in the laboratory might fuel efforts towards *in vitro* embryo production in this species without the need for repeated in vivo oocyte collection. In depth understanding of the biology behind and improvement of assisted reproductive techniques (ARTs) is the only option for preventing the disappearance of functionally extinct species such as the northern white rhinoceros. In vitro follicle development can only be obtained by in depth knowledge on rhinoceros ovarian histology. In addition to known ovarian features, we identified numerous undescribed structural and molecular ovarian characteristics from adult southern white rhinoceros (n=3). Ovarian sections were stained with H&E, PAS or Masson Trichrome and molecular analyses (hyaluronic acid detection, immunohistochemistry and TUNEL assay) were performed to identify proliferation, extracellular matrix, pluripotency markers, hormones, enzymes, markers for inflammation or endocrine glands, blood vessel presence, oocyte markers and apoptosis. Besides degenerating, deformed, or luteinized follicles, analysis revealed several 'follicle-like structures' (FLS) that deviated from the expected follicle appearance. Most importantly, the majority of FLS did not contain any oocyte and were comprised of a collection of cells organised around fluid islands with or without an antral cavity. The discovery and description of FLS in aged southern white rhinoceroses may play a role in poor oocyte recovery rates in ovum pick-up (OPU) in older rhinoceroses. It remains to be investigated whether FLS might be present on ovaries from other rhinoceros species and whether they might serve as a general indicator for oocyte recovery success in aged females.

1. Introduction

The earth's sixth mass extinction, currently in progress, necessitates scientists to find solutions to preserve biodiversity. With 22 % of all mammalian species faced with disappearing from the planet [1], time is running out. When conservation methods such as habitat protection or restoration are insufficient to prevent the loss of keystone species, such as the rhinoceros, complementary actions in the field of assisted reproduction techniques (ART) such as ovum pick up (OPU) and in vitro embryo production and advanced ART such as cloning and stem cell techniques are crucial [1,2]. These state-of-the-art techniques can help in genetic management and the preservation of genetic diversity. However, before such specialised techniques can be applied, a thorough understanding of the species-specific reproductive biology is required. This knowledge of reproduction includes anatomical and physiological analysis [3]. Histology, the microscopic counterpart of gross anatomy, is a valuable tool to study normal and diseased tissue [4]. Light microscopy as well as immunohistochemistry are methods to identify cells and allow to differentiate normal tissue from pathological structures [5].

Studies of rhinoceros reproductive tracts and their ovaries have been extremely limited. In a previous study, we recently sought to address this ovarian knowledge for the southern white rhinoceros deficit and have carried out an in-depth molecular and histological analysis of physiological follicular development using neonatal and adult ovaries [6].

* Correspondence to: Nuffield Department of Women's & Reproductive Health, University of Oxford, Level 3, Women's Centre, John Radcliffe Hospital, Oxford OX3 9DU, United Kingdom.
E-mail address: suzannah.williams@wrh.ox.ac.uk (S.A. Williams).

https://doi.org/10.1016/j.therwi.2024.100096
Received 22 December 2023; Received in revised form 30 May 2024; Accepted 3 June 2024
Available online 4 June 2024

Table 1
Description of the primary and secondary antibodies used in this study.

Primary antibody	Function	Catalogue	Species	Concentration	Secondary antibody	Catalogue	Dilution
collagen I[1]	extracellular matrix protein	MA1–26771	mouse monoclonal	25 μg/ml	goat anti-mouse IgG[4]	BA-9200	1:200
Ki-67[1]	proliferation marker	PA5–19462	rabbit polyclonal	5 μg/ml	goat anti-rabbit IgG[4]	BA-1000	1:200
minichromosome maintenance complex component 2 (MCM2)[1]	proliferation marker	PA5–79645	rabbit polyclonal	2.5 μg/ml	goat anti-rabbit IgG[4]	BA-1000	1:200
sex determining region Y-box 2 (SOX2)[1]	pluripotency factor	PA1–16968	rabbit polyclonal	5 μg/ml	goat anti-rabbit IgG[4]	BA-1000	1:200
octamer-binding transcription factor 4 (Oct4 or POU5F1)[2]	pluripotency factor	11263–1-AP	rabbit polyclonal	3.75 μg/ml	goat anti-rabbit IgG[4]	BA-1000	1:200
DEAD-Box Helicase 4 (DDX4 or Vasa)[1]	germ cell marker	PA5–23378	rabbit polyclonal	5 μg/ml	goat anti-rabbit IgG[4]	BA-1000	1:200
anti-Müllerian hormone (AMH)[1]	hormone indicative for ovarian reserve	PA5–35851	rabbit polyclonal	5 μg/ml	goat anti-rabbit IgG[4]	BA-1000	1:200
cannabinoid receptor 1 (CB1)[2]	G protein-coupled receptor	17978–1-AP	rabbit polyclonal	5.5 μg/ml	goat anti-rabbit IgG[4]	BA-1000	1:200
cluster of differentiate 20 (CD20)[1]	B-lymphocyte marker	PA5–16701	rabbit polyclonal	0.1925 μg/ml	goat anti-rabbit IgG[4]	BA-1000	1:200
cluster of differentiation 31 (CD31)[2]	endothelial cell marker	11265–1-AP	rabbit polyclonal	0.6 μg/ml	goat anti-rabbit IgG[4]	BA-1000	1:200
aromatase[1]	enzyme responsible for biosynthesis of estrogens	PA1–21398	rabbit polyclonal	5 μg/ml	goat anti-rabbit IgG[4]	BA-1000	1:200

Companies: [1] Invitrogen, [2] Proteintech, [3] Abcam, [4] Vector Laboratories.

Previous investigations of rhinoceros reproductive pathology has primarily utilised ultrasound analysis of live individuals [7–12] although this does not enable precise cellular analysis. There has been only one case study that investigated an ovarian adenocarcinoma with metastases in a white rhinoceros using histological analysis [13]. Therefore, in this study we present detailed histological and molecular findings on novel ovarian structures in the southern white rhinoceros. The information provided in this study describes unusual, species-specific, ovarian phenomena that advance our knowledge of the southern white rhinoceros ovary and might influence the use in ARTs in this, and related, species.

2. Material and methods

2.1. Collection of ovarian tissue

Ovarian tissue was collected from three adult southern white rhinoceros (rhino 1 39.5 years, rhino 2 30 years and rhino 38 years of age). Rhinoceroses 1 and 3 were euthanised because of old age and a declining quality of life or health reasons and rhinoceros 2 had its Achilles tendons ruptured during an unexpected mating. After humane euthanasia, the ovaries were dissected, kept on ice and transported to the laboratory at the University of Oxford in the UK (rhino 1 collected in Whipsnade zoo, UK) or the Leibniz Institute for Zoo and Wildlife Research in Germany (rhino 2 and 3 collected in Beekse Bergen, The Netherlands and Salzburg zoo, Austria, respectively). The gross anatomy of the investigated ovaries along with the reproductive history of the rhinoceroses are described in a previous study in which rhino 1, 2 and 3 are respectively named rhino 2, 3 and 4 [6]. In brief, only rhino 1 had a proven fertility since she produced one calf in 2001 and one in 2005. Rhino 2 never produced calves and no reproductive history is known about rhino 3.

2.2. Histology

After arrival in the laboratory, cross sections through the ovary or whole ovaries were fixed for histology and the remainder was cryopreserved. Slices of all rhinoceros ovaries (rhino 1–3) were fixed in either Bouin's fixative, 10 % (v/v) neutral buffered formalin (NBF) or Form-Acetic (NBF with 5 % acetic acid) [14]. Fixed samples were embedded in paraffin wax and sectioned. Allocation of the fixed pieces was carried out as described in Appeltant et al. [6]. Briefly, for rhino 1 and 3 cross sections were collected from both poles and the middle part of the ovary. We only obtained one ovarian pieces of the left and two pieces of the right ovary of rhino 2. Sections were stained either with hematoxylin and eosin (H&E, Hematoxylin solution Gill No. 2, GHS232, Sigma Aldrich; eosin Y solution alcoholic with phloxine, HT110332, Sigma Aldrich; for gross morphology of the tissue section), Periodic acid Schiff stain (PAS; Periodic acid solution, Sigma Aldrich, UK; 3951; Schiff's reagent, Merck, UK; 1.09033.0500; to detect polysaccharides) or with Masson's trichrome stain (Abcam, UK; ab150686; to distinguish cells from surrounding connective tissue).

2.3. Hyaluronic acid detection

To determine the presence of extracellular matrix, hyaluronic acid was detected in paraffinized fixed tissue sections using hyaluronic acid binding protein (HABP) as previously carried out [15,16] with some modifications: 5 μg/ml hyaluronic acid binding protein [17,18] (Calbiochem, Sigma Aldrich 385911) diluted in blocking solution for 2 h at room temperature (RT). Negative controls were treated with blocking solution only. After washing, detection was visualised using the Vectastain ABC Elite kit (Vector laboratories, PK-6100) and a DAB peroxidase substrate kit (Vector laboratories, SK-4100).

2.4. Immunohistochemistry

Immunohistochemistry was performed on fixed sections for the antibody targets described in Table 1. All the antibodies in this study, except for cluster of differentiation 31 (CD31) and aromatase, were used in a previous publication on rhinoceros ovarian histology [6]. In addition to Ki-67, we used MCM2 to detect proliferating cells, such as infrequently dividing granulosa cells in early pre-antral follicles [19]. Following dewaxing and rehydration, a heat-induced (microwave: 1 min high power, 9 min medium power), low pH antigen retrieval using sodium citrate (pH 6.0) was applied for collagen I, Ki-67, MCM2, SOX2, DDX4, aromatase and CD20. For Oct4, AMH, CB1 and CD31 the antigen retrieval method was heat-induced high pH by Vector antigen unmasking solution (Vector Laboratories, H-3301). Sections were submerged in 3 % hydrogen peroxide for 5 min at room temperature to block endogenous peroxidase activity. To prevent non-specific binding, sections were incubated in 5 % normal goat serum (NGS; Vector). Hereafter, sections were incubated in primary antibodies for 2 hours at room temperature; for negative controls, the primary antibody was

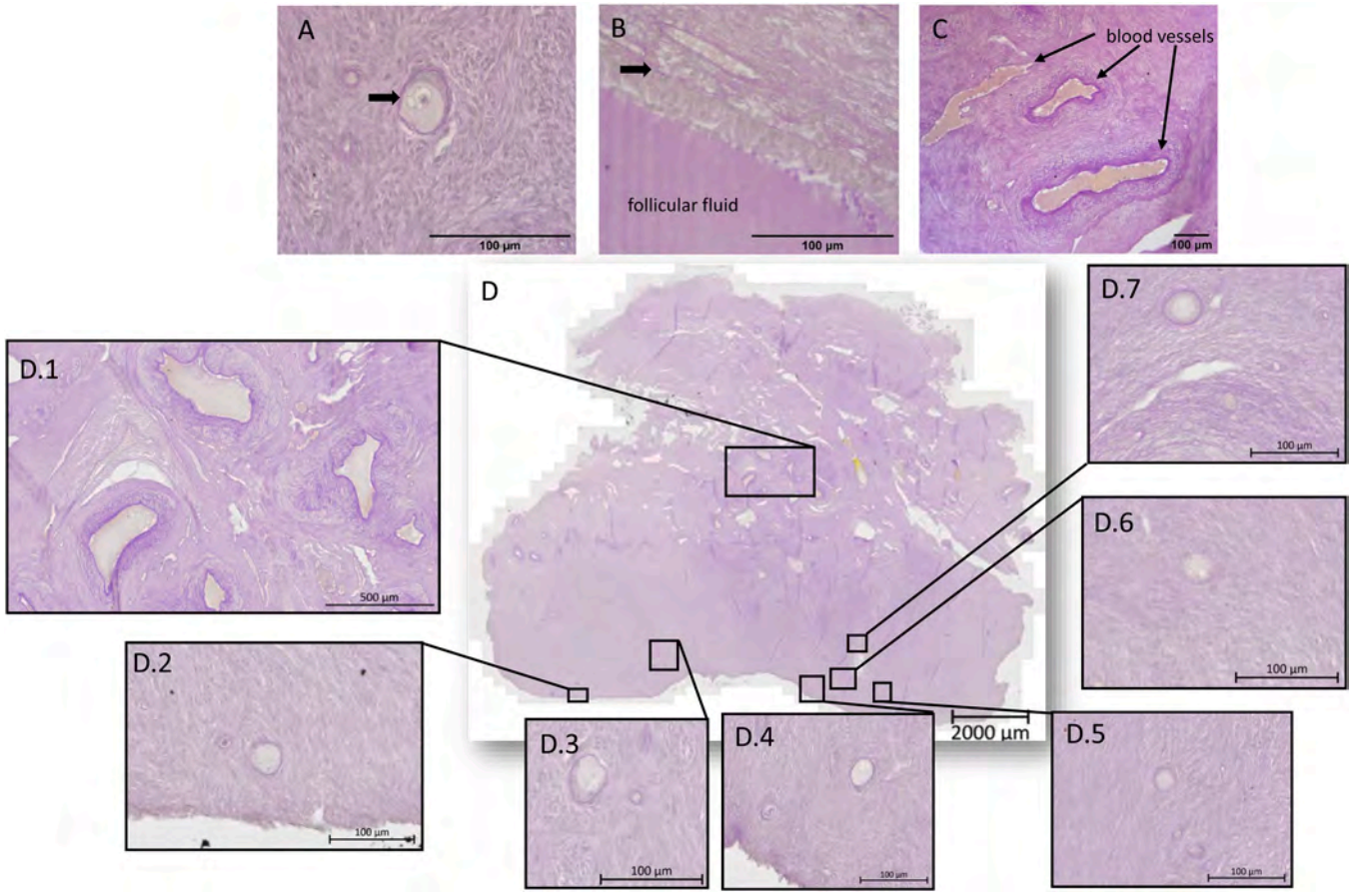

Fig. 1. Periodic acid–Schiff staining (PAS) of ovarian sections of an adult southern white rhinoceros. Several structures are strongly positive for polysaccharides highlighted by PAS such as the basal membrane of follicles (A and B; indicated by a thick black arrow), follicular fluid (B), and the wall of blood vessels (C). (D) Analysis of location and structure of follicles in an ovarian section. (D.1) Medullar region containing mainly stroma and blood vessels. (D.2 to D.7) Early stage follicles (transitional and secondary) in the cortex.

omitted. Samples were incubated in secondary biotinylated antibodies as described in Table 1 for 1 hour at room temperature. Detection was visualised using the Vectastain ABC Elite kit followed by DAB (as above). For all antibodies, slides were counterstained with Hematoxylin solution Gill No. 2 (as above).

2.5. TUNEL assay

To detect double-stranded DNA breaks, the FragEL™ DNA fragmentation detection kit (Merck Millipore, QIA33) was used according to the manufacturers' instructions.

2.6. Microscopy

The results of histology, HABP, immunohistochemistry and TUNEL staining were analysed using a light microscope (Leica DM2500). Pictures were captured by the Lumenera Infinity 5 camera with accompanying Infinity Analyze software (Teledyne Lumenera, Nepean, Canada). Scanned images were obtained by the high performance bright-field slide scanner ZEISS Axioscan 7 at magnification 20x.

2.7. Ovarian follicle classification

Follicles were classified according to established criteria [14,20,21] in the following groups: primordial (oocyte surrounded by a single layer of flattened pre-granulosa cells), transitional (mixed layer of flattened and cuboidal granulosa cells surrounding the oocyte), primary (single layer of cuboidal cells surrounding the oocyte), secondary (two layers of cuboidal granulosa cells surrounding the oocyte), pre-antral (many granulosa cell layers without or with interspersed fluid filled areas) and antral (many layers of granulosa cells and a large antral cavity) follicles.

3. Results and discussion

3.1. Follicle classification

Overall, the ovaries of the three rhinoceroses appeared to be in a quite inactive state since they did not shown the presence of multiple macroscopically visible, large antral follicles. Histological examination of three adult white rhinoceros ovaries identified follicles in several stages of development from a primordial (Fig. 1A) to a large antral follicle (Fig. 1B). The PAS staining highlighted the basal membrane and blood vessels (Figs. 1C and 1D.1). The follicular fluid in antral follicles also stained purple indicating the presence of secreted polysaccharides (Fig. 1B). A scanned adult ovary section contained six follicles in the cortical region ranging in development from a transitional to a secondary stage follicle (Fig. 1D.2 to 1D.7). For an in-depth description of follicle development in the southern white rhinoceros, see Appeltant et al. [6].

3.2. Remarkable structures

Besides normal physiological structures, various formations that were not readily recognisable as normal ovarian structures, were identified. By performing histology, hyaluronic acid detection, immunohistochemistry to analyse the molecular characteristics of these abnormal

Table 2
Overview of the main characteristics in the remarkable structures of this study.

	Fluid filled tissue mass	Follicle-like structure	Deformed follicle	Formation of corpus luteum	Degenerating follicle	Cells at the transition of the cortex and medulla
Presence of oocyte	no	no or degenerated	yes	no	no	no
Antrum	+	+	+	+	+	-
Call-Exner bodies	NA	+	NA	NA	NA	NA
PAS	NA	+	NA	-	NA	-
Hyaluronic acid	NA	+	NA	-	+	-
TUNEL	NA	normal	normal	normal	normal	NA
Collagen I	NA	NA	NA	NA	NA	-
Ki-67	NA	normal	-	normal	low	-
MCM2	NA	normal	-	normal	low	-
SOX2	NA	NA	+	+	NA	NA
Oct4	NA	NA	-	-	NA	NA
DDX4	NA	NA	NA	NA	NA	-
AMH	NA	+	NA	-	NA	NA
CB1	NA	-	-	+	NA	-
CD20	NA	NA	-	NA	NA	NA
CD31	NA	-	-	+	NA	NA
Aromatase	NA	NA	+	-	NA	NA

NA: not applicable, which refers to not being tested.
PAS: Periodic acid solution; MCM2: minichromosome maintenance complex component 2; SOX2: sex determining region Y-box 2; Oct4: octamer-binding transcription factor 4; DDX4: DEAD-Box Helicase 4; AMH: anti-Müllerian hormone; CB1: cannabinoid receptor 1; CD20: cluster of differentiate 20; CD31: cluster of differentiation 31.

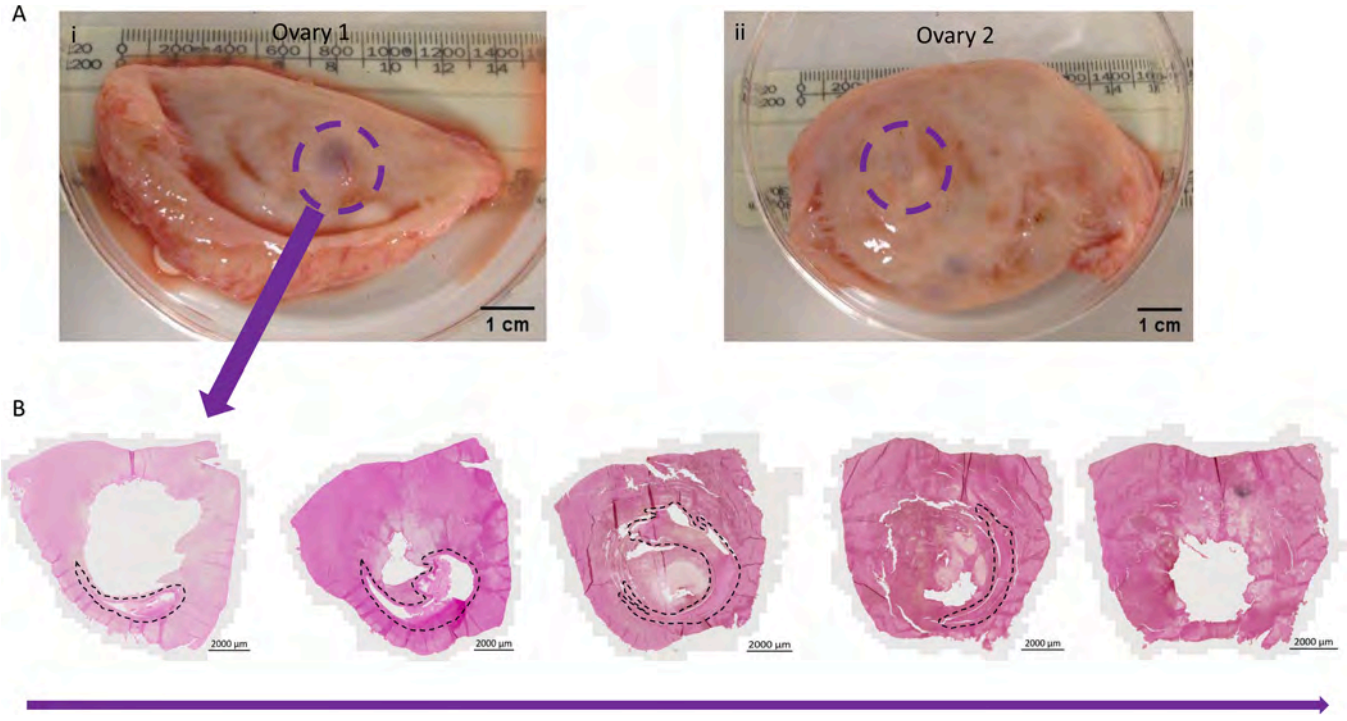

Fig. 2. Ovarian tissue mass compressed presumed antral follicle in adult southern white rhinoceros ovary. (A) Macroscopic appearance of the ovary containing the structure illustrated in B. The dashed line in A.1 outlines the borders of the B structure isolated from ovary 1. Ovary 2 contained a similar structure (dashed line in A.2). (B) From left to right following the arrow the area surrounded by a dashed line is outlining a presumed antral follicle although no oocyte could be found. The third image is clearly showing that the follicle is compressed by an ovarian tissue mass.

structures and TUNEL, we have verified differential diagnoses for six of those structures (Table 2).

3.2.1. *Fluid filled tissue mass*

While dissecting the ovaries of rhino 1 (Fig. 2A), a presumed antral follicle was isolated separately (Fig. 2Ai and 2Aii dashed lines). However, upon histological analysis of the presumed follicle presented in 2Ai, it was revealed that the isolated structure was not entirely occupied by an antral follicle as no oocyte was ever found, and the presumed follicle antral space was partially displaced by a fluid filled tissue mass (Fig. 2B). We did not proceed to identify the origin of the tissue mass because this did not fit within the scope of this study.

3.2.2. *Follicle-like structures*

Histological analysis of rhino 2 and 3 revealed several follicle-like structures (FLS) that resembled follicles, but they deviated from the

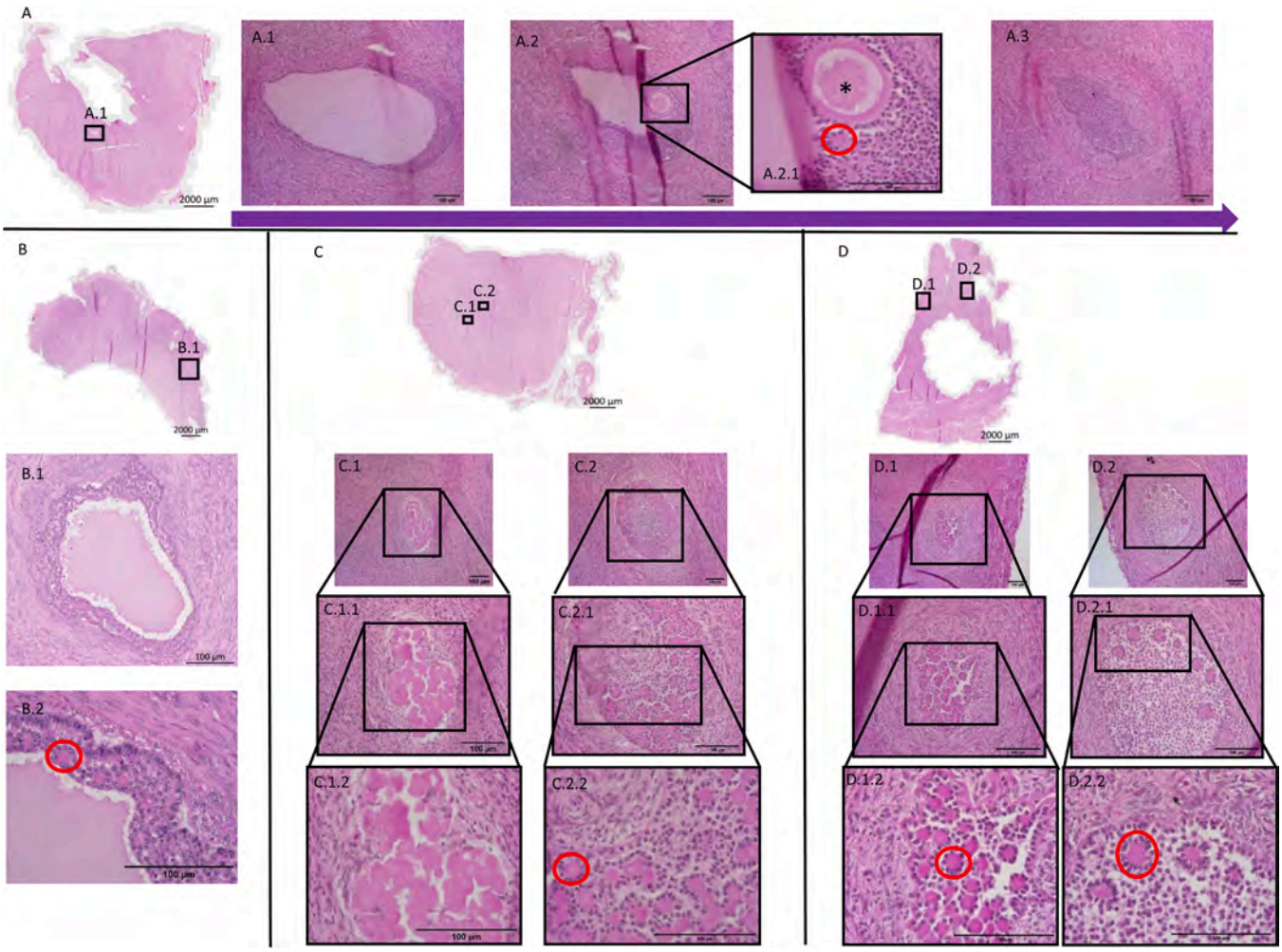

Fig. 3. Characterisation of unknown structures named as 'Follicle-like structures' (FLS) observed in adult southern white rhinoceros ovaries (n=2). (A) Scanned image of an ovarian tissue piece containing a FLS containing an oocyte. A.1 till A.3 are detailed images of sequential sections through a FLS. A.2.1 is a magnified image of the oocyte (asterisk) found in section A.2. (B) Scanned image of an FLS detailed in B.1 and in B.2. (C) Scanned image of the ovary containing two FLS: C.1 and C.2., which are detailed in higher magnifications in C.1.1 and C.2.1 and C.1.2 and C.2.2. (D) Scanned image of two FLS (D.1 and D.2). D.1.1 till D.2.2 are detailed images at higher magnifications to present the structure of the FLS. Examples of 'Call-Exner bodies' which are spherical eosinophilic regions surrounded by a rosette of granulosa cells are indicated by a red circle. Except for the scanned overviews, all the scale bars represent 100 µm.

expected appearance. These FLS were built up out of a collection of granulosa-like cells organised around fluid islands with or without an antral cavity (Fig. 3A to 3D). No living oocytes were ever detected in FLS, only once a degenerated oocyte was found in an FLS (Fig. 3A.2.1, asterisk).

After an initial histological evaluation based upon an H&E staining, the FLS were potentially highly vascularized neoformations, more specifically, aggressive granulosa cell tumours. In rhino 3, sections through the middle (Figs. 3C and 3D) as well as towards one pole (Fig. 3A) of one ovary contained these abnormal formations. In rhino 2 we only discovered two FLS (Fig. 3B and Fig. 4A), one in each ovary. In those animals, we did not often observe a healthy antral follicle containing an oocyte, but we did encounter some small pre-antral follicles. Some of those follicles in rhino 2 are described in Appeltant et al. [6]. The follicular origin of FLS was confirmed by one formation still containing a degenerated oocyte (Fig. 3A.2 overview and 3 A.2.1 detail).

Although, in the majority of cases, no oocytes were observed, the structures fulfilled all the expected H&E (Fig. 4A), PAS (Fig. 4B) and HA (Fig. 4C) criteria to call a structure a follicle [6]. PAS clearly highlighted the follicular basal membrane (Fig. 4B, red arrow), and some anti-Müllerian hormone (AMH) positivity (as compared to the negative control inset) as a granulosa cell identifier was detected (Fig. 4D). In 2010, a metastatic uterine adenocarcinoma was described in a southern white rhinoceros [22] and in 2021, a brief report was published on an ovarian adenocarcinoma with histological description [13], but no granulosa cell tumours were described yet. Since there is no specific marker for granulosa cell tumors, diagnosis was based on extensive molecular characterisation using a panel of antibodies [23]. The proposed identification of granulosa cell tumours in our samples was based upon the localization of the aberrant cell formation (within a follicle structure) and the appearance of Call-Exner bodies. One of the characteristic pathological features of a granulosa cell tumour is the formation of these Call-Exner bodies that are small cystic areas filled with fluid and cellular debris aligned by differentiated granulosa cells [24], which resembled the fluid islands identified in the FLS.

To investigate the vascularisation pattern in the proposed neoformation, we detected CD31, which showed no vascularisation in the structure at all (Fig. 4E). This observation together with the hyaluronic acid positivity of the fluid islands (Fig. 4C) led us to conclude the fluid was follicular fluid. Despite the neoformation indicator such as the hyalinised cores, the absence of excessive proliferation (associated with tumour characteristics) as detected by Ki-67 (Fig. 4F) or MCM2 (Fig. 4G) resulted in us exploring other options to identify these structures. Interestingly, detecting Ki-67 emphasized a circle of proliferative cells

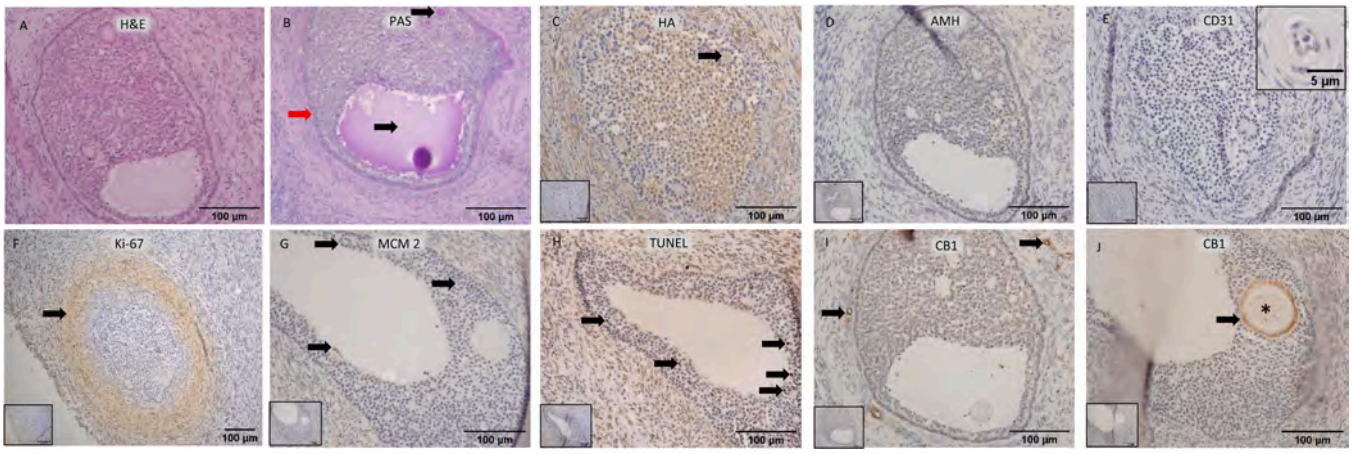

Fig. 4. Histological and molecular characterisation of follicle-like structures (FLS) in adult southern white rhinoceros ovarian sections. (A) Section stained with haematoxylin and Eosin (H&E). (B) Section stained with Periodic acid Schiff stain (PAS). Black arrows indicate PAS positive regions and the red arrow points towards the basal membrane. (C) Detection of Hyaluronic acid (HA). The black arrow indicates HA positive fluid in a Call-Exner body. (D) Detection of anti-Müllerian hormone (AMH). (E) Detection of cluster of differentiation 31 (CD31) with in the right upper corner an inset image of a positive control of which the endothelial cells are positive. (F) Detection of proliferation marker Ki-67. Instead of focussed nuclear detection there is a Ki-67 positive blur around the FLS (black arrow). (G) Detection of proliferation marker minichromosome maintenance complex component 2 (MCM2; positive cells are indicated by black arrows). (H) Apoptotic TUNEL positive cells are indicated by black arrows. (I and J) Detection of cannabinoid receptor 1 (CB1); overview of the FLS and location of the oocyte (asterisk). Blood vessels as well as the oocyte zona show a positive signal (black arrows). Inset images are negative controls.

around the FLS (Fig. 4F, black arrow). To exclude a process of degeneration, a TUNEL assay was performed, but only a few sporadic cells were apoptotic (Fig. 4H).

A second hypothesis was that the FLS structures might be defined as interstitial glands of the ovary. This term refers to interstitial cells that might be producing a variety of steroids such as estrogens, progesterone and androgens; however no physiological evidence has been provided yet [25]. According to aetiology of interstitial glands, the cells can be divided into seven categories: foetal, thecal, stromal, gonadal-adrenal, adneural, medullar-cord and rete [26]. The amount and morphology of the interstitial glands is varying considerable according to the physiological state of the ovary and is not correlated to the specific origin category [26]. Across species the manifestation of the interstitial glands may go from unnoticeable to large masses [26]. In Iraqi buffaloes, interstitial glands can manifest as simple cuboidal epithelium containing many lumens of secreting glands, which resembles the fluid islands in our study [27]. As an indicator for interstitial glands, we used the cannabinoid receptor 1 (CB1). In adult mice, CB1 has been discovered in progesterone-producing cells of ovarian interstitial glands [28], and in the rat ovary, CB1 has been demonstrated in the ovarian surface epithelium, the granulosa cells of antral follicles and the luteal cells of functional corpora lutea [29]. It is known that endocannabinoids influence reproduction from gametogenesis to pregnancy [30]. The fact that CB1 is localised in mitochondria, the place where progesterone is produced, might indicate that endocannabinoids modulate progesterone synthesis through CB1 [28]. The FLS did not show any positive CB1 signal, but the blood vessels around the structure and the zona pellucida of the oocyte present in one of the FLS showed a strong signal (Figs. 4I and 4J). Although not present in rat oocytes, human oocytes are also expressing CB1 [29]. The presence of CB1 in blood vessels has not been described for other species and is therefore a new observation for the rhinoceros. A previous study found cannabinoid receptor 2, but not 1, in blood vessels of the gastrointestinal tract of dogs [31]. However, CB1-immunoreactive neurons were detected in the submucosal blood vessels of the porcine enteric system [32] thus providing evidence blood vessel can appear CB1 positive.

Since the FLS didn't contain a healthy oocyte, they might have been considered some kind of cysts. Ovarian cysts can be categorised according to the type and morphology of lining cells and the tissue they are embedded in [33]. Since FLS consisted out of granulosa-like cells which mostly still appeared in a cuboidal state and were surrounded by theca-like cells, connective tissue and blood vessels, we hypothesized follicular cysts. However, cyst are normally described as having thin walls in contrast to the thick walled structures we observe. In addition, the fluid organises more like small filled spaces surrounded by granulosa cells in contrast to distended fluid-filled spaces. In general, a cyst is considered an anovulatory structure that surpasses the ovulatory size [34], which was not observed in our samples, but it was suggested that cysts can undergo dynamic changes where they increase and decrease in size [34]. In the southern white rhinoceros, to date, mostly para-ovarian cysts have been described [9,35]. Therefore, although we could not exclude cysts with certainty, cystic formation is unlikely and there were no strong arguments to define FLS as ovarian cysts.

Since both a pathological cause and interstitial glands seemed to be unlikely, we conclude that FLS's were a type of physiological state of follicles. Since normal follicles were also observed in the same individual (rhino 3) and other samples (rhino 1), we prefer to use the term follicle-like structure (FLS) until more insight will be obtained about its true nature and functionality. Similar structures containing foci or pockets of follicular fluid accumulating between granulosa cells have been observed during the antral follicle formation in bovine and mouse [36]. During antrum formation, granulosa cells will move relative to each other and in the centrally located granulosa cells there might even be cell death involved to allow follicular fluid to accumulate [36]. Although Call-Exner bodies are considered pathognomonic for human granulosa cell tumours, in the rabbit the terminology is used to indicate the physiological fluid-filled cavities between granulosa cells of small antral follicles before they all coalesce into a large antrum [37]. This emphasises the fact that the appearance of such smaller fluid-filled foci might be species-specific and therefore, the rhinoceros can be added alongside the rabbit, human, guinea-pig, monkey, sheep and bovine species in the list of species showing this phenomenon [38].

The most remarkable feature about the FLS was the absence of a healthy oocyte in any of our samples. Only one FLS contained a degenerated oocyte. Regardless of the unknown physiological role of these FLS, they might have serious implications while performing ART such as OPU on those ovaries. It is reported that the oocyte recovery rate, defined as the number of retrieved oocytes in relation to the number of punctured follicles during OPU, in the white rhinoceros is relatively low compared to other species [39]. In the rhinoceros, oocyte recovery rates

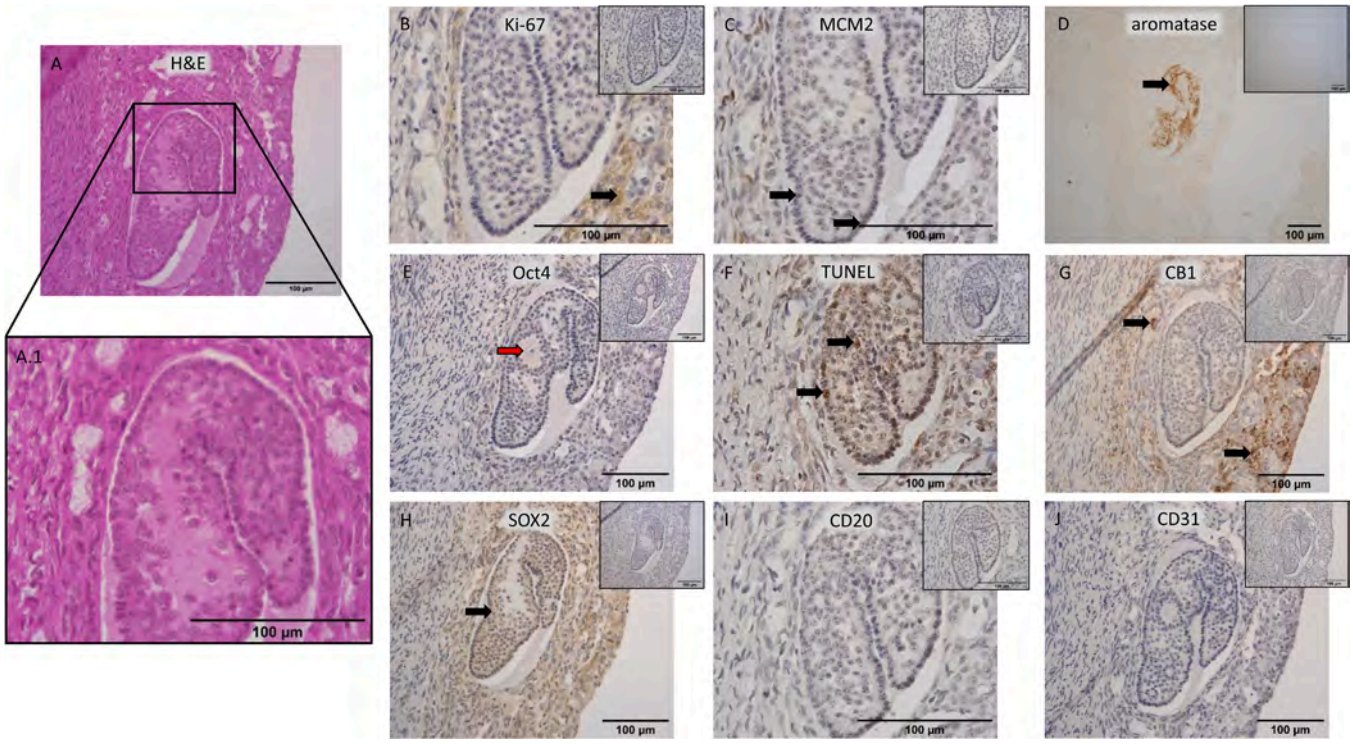

Fig. 5. Molecular characterisation of a deformed follicle in the ovary of an adult southern white rhinoceros. (A) Haematoxylin and Eosin (H&E) staining with detail (A.1). (B) Proliferation markers Ki-67 and (C) minichromosome maintenance complex component 2 (MCM2) showed minimal cellular proliferation in the follicle. (D) Aromatase positive granulosa cells (black arrow). (E) All the cells in the follicle are Oct4 negative and the oocyte could be seen (red arrow). (F) Several TUNEL positive cells could be observed in the wall of the follicle (black arrow) indicating apoptosis. (G) Cannabinoid receptor 1 (CB1) positive cells were present around, but not within the follicle. (H) All the granulosa cells showed a positive signal for sex determining region Y-box 2 (SOX2). (I) No CD20 positive cells could be detected. (J) The structure was CD31 negative and therefore not situated intravascularly. Inset images are negative controls.

of only 26.4 % [40] and 34.4 % [39] are obtained while in horses numbers exceed 50 % [41,42] and in cattle, rates of 70.9 % [43] and 75 % [44] have been reported. The discrepancy between the aspiration and oocyte recovery rates during OPU in the white rhinoceros might be linked to the presence of FLS in addition to a suspected failure of ovarian super-stimulation prior to OPU, lack of mechanical scraping of the follicular wall or technical failure of oocyte aspiration during OPU [39]. FLS without oocytes cannot be differentiated during ultrasound prior to aspiration, but might contribute to low oocyte recovery rates. In female rhinoceroses ≥25 years no oocytes could be retrieved in half of the OPU sessions compared to younger animals (≤24 years) where only 6 % of the OPU sessions failed to provide oocytes [39]. When samples would be available, it would be interesting to verify whether young animals also show the presence of FLS to investigate their influence on recovery rates after OPU. The sizes of the FLS are quite small when considering normal ultrasound procedures. However, we believe these structures can still grow in size since TUNEL staining did not show high levels of apoptosis and Ki-67 indicated an active proliferation zone around the FLS. The fact that we observed for the first time, to our knowledge, these FLS in two old individuals might indicate that this is a typical age-related phenomenon for the southern white rhinoceros. However, since the FLS appeared in rhino 2 (never had a calf) and rhino 3 (no reproductive history known), but not in rhino 1 which was the oldest, but proven fertile one, the FLS phenomenon might be related to possible subfertility/infertility regardless of age.

3.2.3. *Deformed follicle*

When first observing the structure illustrated in Fig. 5, besides being a deformed follicle (Fig. 5A.1), an intravasal located cell formation, most likely a neoformation or tumour described as an intravascular leiomyomatosis, was also considered. In human, an intravascular leiomyomatosis is a rare benign condition in which smooth muscle cells proliferate within blood vessels [45]. The origin of the proliferating smooth muscle cells are the uterine venous wall or a uterine myoma [45]. Leiomyomas are also found in rhinocerotidae such as the white, Sumatran and Indian species although the white rhinoceroses studied (i.e., in captivity) have a higher prevalence of other reproductive pathologies such as ovarian cysts [7,9]. Leiomyomas of the reproductive tract and cystic hyperplasia represent 80 % of the most common pathologies in non-reproductive female rhinoceros and elephants [46]. Since we collected samples from zoo animals undergoing long-term captivity, these can be symptoms of asymmetric reproductive aging, a term referring to the premature reproductive senescence due to prolonged periods of sex steroids from continuous ovarian cyclic activity in non-reproducing females [46]. However, since the ovarian structure was negative for both Ki-67 (Fig. 5B) and MCM2 (Fig. 5C), both indicators of proliferation, and expected to be raised in neoformations [47], the possibility of an intravascular leiomyoma was excluded. The aromatase activity (Fig. 5D) could indicate active granulosa cells [48] and an oocyte was observed (Fig. 5E, red arrow), but no well-defined antrum was present. In order to explain the unusual morphology, we investigated cell death by TUNEL (Fig. 5F), but there was no generalised degeneration. Since interstitial glands can take many different forms [26], we tested CB1, but the structure was negative unlike cells around it which were strongly positive (Fig. 5G). Interestingly, the entire entity was embedded in the wall of a larger structure with a central large lumen (Fig. 6) although both had some distinct features as illustrated by the aromatase (Figs. 5D and 6H) and CB1 (Figs. 5G and 6G) immunoreactivity. Both structures were moderately positively reacting for SOX2 (Fig. 5H), indicating some pluripotency. However, this pluripotency was not confirmed by Oct4 detection (Fig. 5E). This is in line with the observation of a study in the pig in which isolated granulosa cells expressed stemness markers such as Nanog and SOX2, but no Oct4 [49]. Another possibility for this structure would be an intravascular B cell

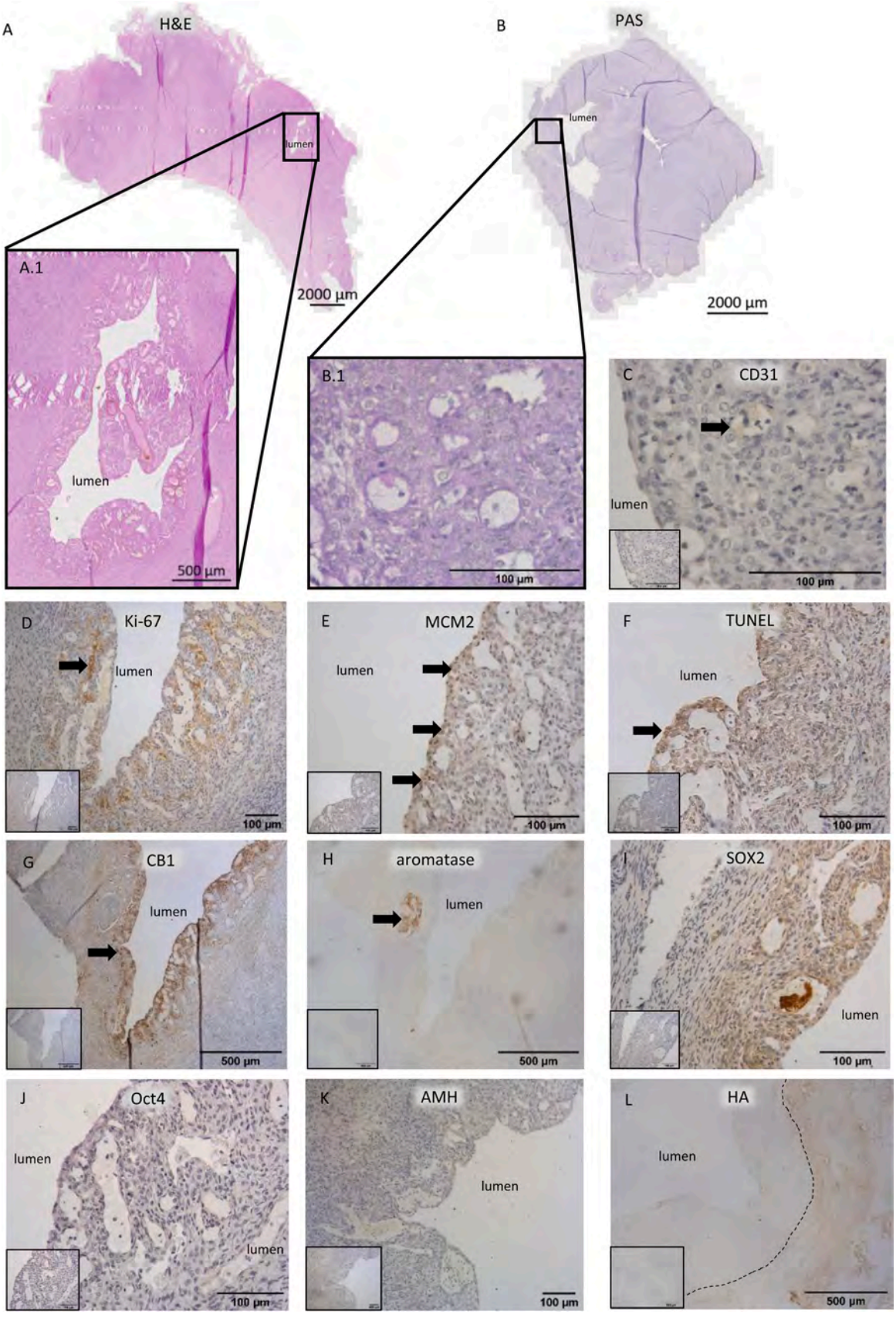

(caption on next page)

Fig. 6. Molecular characterisation of lumen structures in the ovary of an adult southern white rhinoceros. (A) Scanned Haematoxylin and Eosin (H&E) section with higher magnification of the lumen (A.1). (B) Scanned Periodic acid Schiff stain (PAS) section with higher magnification of cells adjacent to the lumen (B.1). (C) CD31 indicated some smaller blood vessels in the wall of the lumen structure. (D) A large number of cells in the wall were positive for the proliferation marker Ki-67 positive. (E) Numerous cells lining the lumen were positive for the proliferation marker minichromosome maintenance complex component 2 (MCM2). (F) Only a few sporadic cells were TUNEL positive. (G) The wall of the lumen structure was cannabinoid receptor 1 (CB1) positive (black arrow). (H) The wall of the lumen structure was aromatase negative. An aromatase positive deformed follicle was bordering the wall (black arrow). (I) The wall of the lumen structure was sex determining region Y-box 2 (SOX2) positive and Octamer-binding transcription factor 4 (Oct4) negative (J). (K) Cells were anti-Müllerian hormone (AMH) negative. (L) The structure was devoid of hyaluronic acid (HA) (left side of the dashed line). Inset images are negative controls.

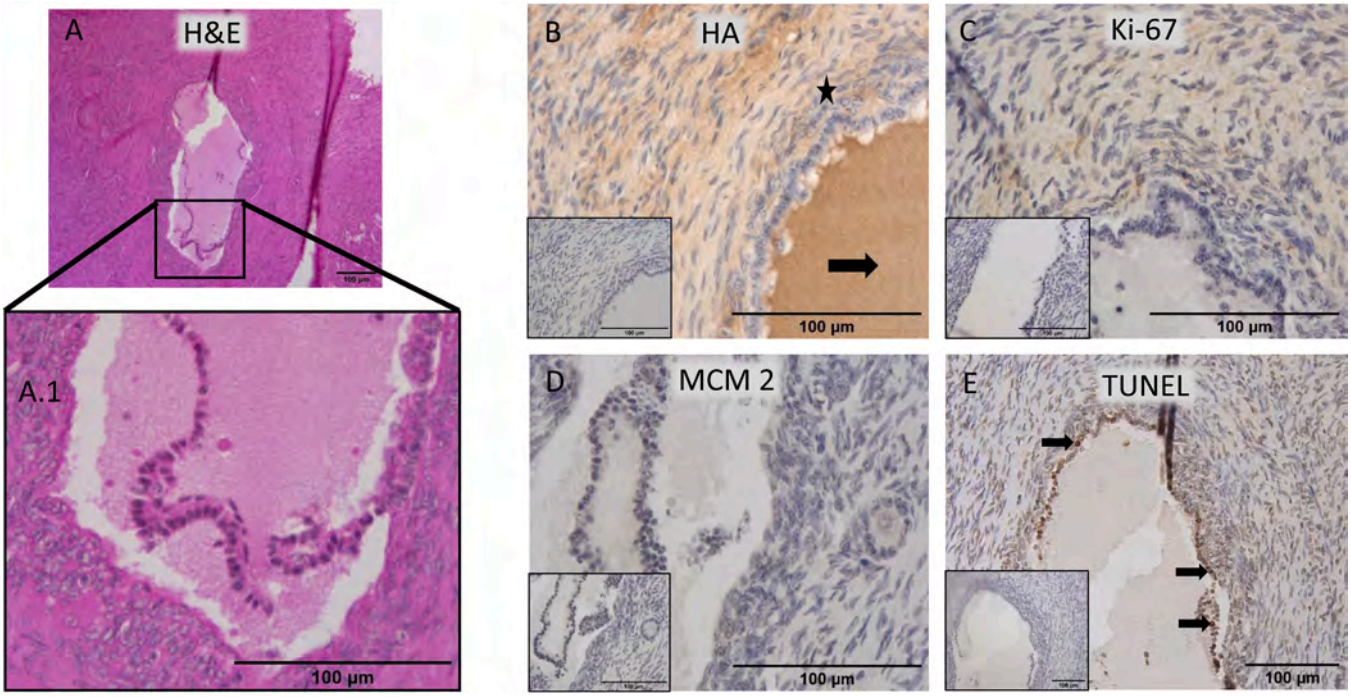

Fig. 7. Molecular characterisation of a degenerating follicle in the ovary of an adult southern white rhinoceros. (A) Haematoxylin and Eosin (H&E) staining with higher magnification panel (A.1). (B) Hyaluronic acid (HA) detection. The black arrow shows the positive follicular fluid area. The star indicates swollen theca interna cells. (C) Proliferation markers Ki-67 and (D) minichromosome maintenance complex component 2 (MCM2) showed no active proliferation. (E) Several TUNEL positive cells could be observed in the wall of the follicle (black arrow) indicating apoptosis. Inset images are negative controls.

lymphoma, but then the cells should have been CD20 positive [50], which was not the case (Fig. 5I). The fact that the structure did not show any positive CD31 signal also confirmed that it was not located within a blood vessel (Fig. 5J). Taking together all these results, we conclude that this is probably a manifestation of a preantral follicle with a deformation that can be described as an invagination.

3.2.4. *Formation of corpus luteum*

As mentioned in the previous paragraph, a preantral follicle with invagination was embedded in the wall of a larger structure containing a central large lumen (Fig. 6, rhino 2). This kind of large structure was observed in the left as well as the right ovary of rhino 2 The wall of the structure was a quite thick layer of a heterogeneous collection of cells of which some showed a balloon-kind of aspect (Fig. 6A.1). Since the samples were collected from aged animals, multinucleated macrophage giant cells associated with inflammation and fibrosis [51] were a possibility. However, multinucleated macrophage giant cells would have been PAS positive because of their phagocytic function [51], which was not the case (Fig. 6B.1). The detection of CD31 revealed that some spaces in the wall were blood vessels (Fig. 6C) rather than balloon-kind of cells (Fig. 6B.1). Detection of Ki-67 (Fig. 6D) and MCM2 (Fig. 6E) revealed the large structure contained proliferating cells, but few apoptotic cells as determined by TUNEL (Fig. 6F). In contrast to the follicle of Fig. 5, this structure was strongly CB1 positive (Fig. 6G) and aromatase negative (Fig. 6H) which together indicated progesterone producing cells. In addition, the cells showed a pattern of SOX2 positivity (Fig. 6I) and Oct4 negativity (Fig. 6J) which could indicate granulosa cells origin. Therefore, the cells could possibly be part of a forming corpus luteum consisting out of luteinizing granulosa cells which are AMH negative, as observed (Fig. 6K). In addition, the structure was lacking hyaluronic acid (Fig. 6L). The overall morphology of a wall bordering a large lumen is quite unusual for a corpus luteum. In the southern white rhinoceros there are two types of corpora lutea described [11]: the first one is a corpus hemorrhagicum where the collapsed follicle fills with blood; the second one, it is a uniform structure as viewed via ultrasonography appearing to lack the blood clot formation phase [11]. The structure we described here, might be a transitionary formation after ovulation towards a uniform corpus luteum. This suggestion is supported by the fact that in the southern white rhinoceros, faecal progestin rise following ovulation is considerably delayed [11], which might indicate a slow formation of the corpus luteum. Another possibility is the formation of a luteinized unruptured follicle since we observed luteinisation of the granulosa cells, the intrusion of small blood vessels and an antral cavity. This can be evoked by certain contraceptive drugs such as low molecular weight follicle-stimulating hormone receptor agonists, and can occur in 5–10 % of the cycles of normal cycling women [52]. In a mouse model generating oocytes lacking *N*- and *O*-glycans, the modified oocytes are not generating anti-luteolytic signals prior to ovulation resulting in premature luteinisation of granulosa cells [53]. Combining these observations, we propose these cells were

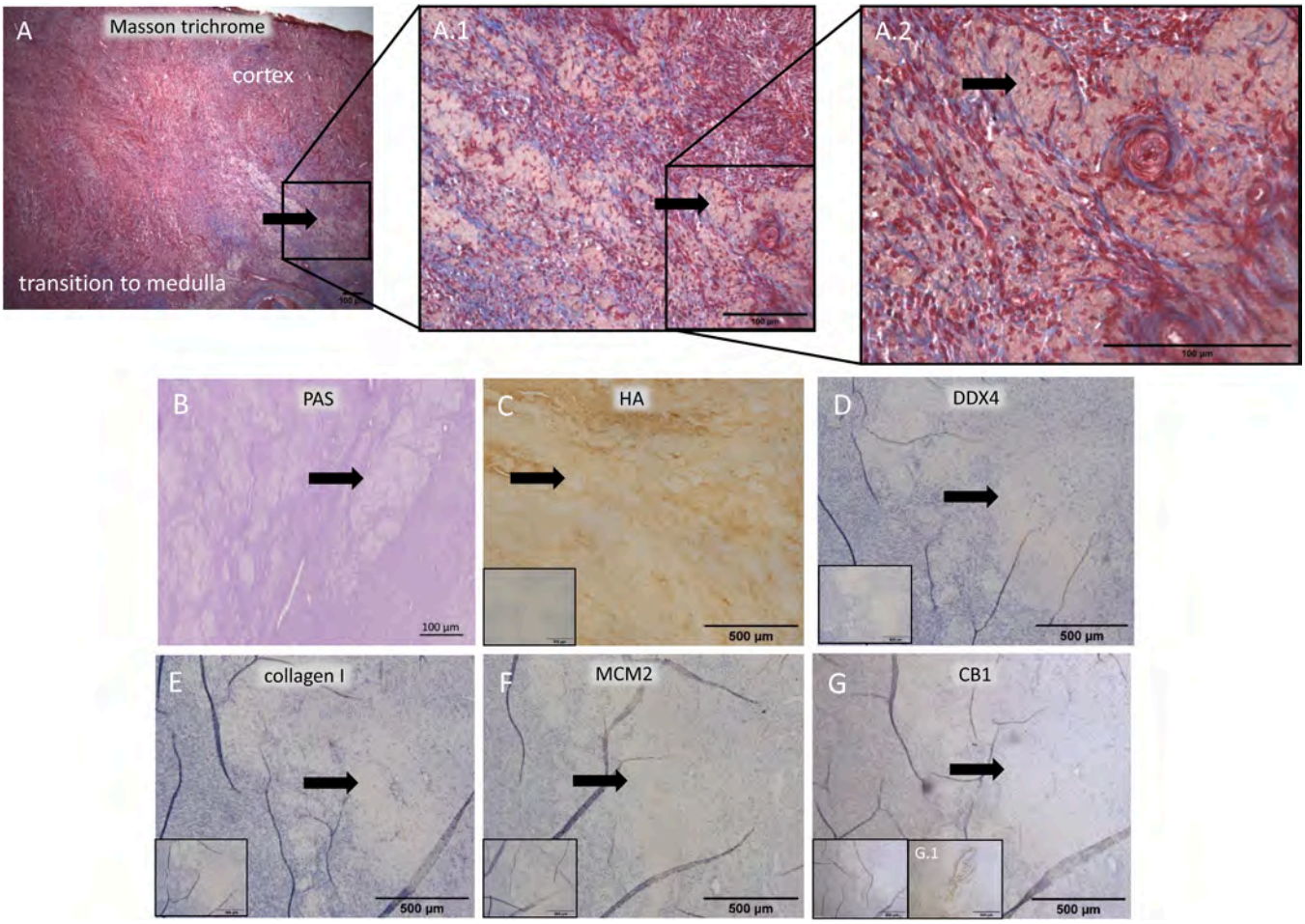

Fig. 8. Illustration of a cell population located on the transition of cortex and medulla of adult southern white rhinoceros ovarian tissue. (A) Masson's Trichrome staining of the transition area between cortex and medulla. (A.1) higher magnification detail of the squared area in A. (A.2) Further higher magnification detail of the squared area in (A.1). (B) Transitionary cells are negative for Periodic acid Schiff stain (PAS) (black arrow). (C) Transitionary cells were negative for hyaluronic acid (HA) (black arrow). (D) Transitionary cells were negative for DEAD-Box Helicase 4 (DDX4, germ cell marker) (black arrow). (E) No collagen I was present between the transitionary cells (black arrow). (F) minichromosome maintenance complex component 2 (MCM2) showed no proliferating cells (black arrow). (G) Transitionary cells were negative for CB1 (cannabinoid receptor 1; black arrow). As a positive control we included the CB1 signal in the blood vessel situated in the medullar region of the ovary to illustrates the immunoreactivity of the sample. Inset images are negative controls.

luteinizing granulosa cells, which could be involved in the development of a uniform corpus luteum or an unruptured follicle.

3.2.5. *Degenerating follicle*

A fluid filled cavity that resembled a follicle was also found in rhino 2, but no oocyte was located in all sections analysed (Fig. 7A). Hyaluronic acid was detected in the fluid of this structure, indicative of follicular fluid (Fig. 7B). With the absence of an oocyte, and what appeared to be swollen theca interna cells (Fig. 7B, star), this led to the differential diagnosis of a follicular cyst [54]. Extremely low proliferation rates (Figs. 7C and 6D) were consistent with the cyst hypothesis. However, this would normally accompany low apoptotic rates [55], which was not the case. Since many TUNEL positive cells were present within the follicle, we expected the structure to be a degenerating follicle rather than a cyst and we hypothesize the oocyte was the origin of the degeneration (Fig. 7E).

3.2.6. *Cells at the transition of the cortex and medulla*

A collection of 'unidentified cells' situated on the transition of cortex and medulla with offshoots into the cortex was observed (Fig. 8) in rhino 1 (ovary 1) and rhino 2 (left ovary). The cells showed a lighter aspect in the Masson Trichrome staining compared to the stromal cells surrounding them (Fig. 8A.1 and 8 A.2). Although the exact mechanism of the red stain is unknown, acid addition during the staining procedure results in less permeable structures retaining the red dye while it is removed from fibers. Therefore, it seems the cells of interest were more permeable than the surrounding stromal cells. The cells were PAS (Fig. 8B), HA (Fig. 8C) and DDX4 (Fig. 8D) negative with no detectable collagen I (Fig. 8E). With no cell proliferation (Fig. 8E), it was not an expanding cell population. The cells did not show any positive CB1 signal (Fig. 8G) so the hypothesis of interstitial glands could also be eliminated. Considering the lack of immunopositivity to the numerous antigens tested, to establish that molecular analysis was possible, we detected CB1 in blood vessels [56] as a positive control (Fig. 8G.1). These unidentified cell formations on the cortex-medulla transition look similar to luteotropic cells derived from luteinized follicles and therefore could be considered the remains of corpora albicantia; regressed corpora lutea. Since these were adult ovaries, other clear presentations of corpora albicantia were present (Suppl Fig. 1A) and thus to verify this hypothesis, 'standard' corpora albicantia were used to compare. Characterisation of the corpus albicantia showed no active cell death (Suppl Fig. 1B) nor an abundance of proliferation of cells (Suppl Figs. 1C and 1D), but it contained a small accumulation of HA (Suppl Fig. 1E), and some cells positive for SOX2 (Suppl Fig. 1F) and Oct4 (Suppl Fig. 1G) in the centre of the structure. The appearance of a cluster of cells with expression of stemness factors has not previously been reported. It is

known that corpora albicantia contain fibroblasts organised in and behaving like a syncytial structure through gap junctions [57], but to our knowledge, the presence of cells with pluripotent characteristics has not been described before in corpora lutea or albicans. CD31 demonstrated the presence of blood vessels in the core of the corpus (Suppl Fig. 1H). No inflammatory cells (CD20, Suppl Fig. 1I) or hormone producing cells (CB1, Suppl Fig. 1J) were detected.

In bovine corpora lutea, the predominant collagen is type I [58], which was not detected in our samples (Fig. 8E). However, the collagens present in corpora lutea might be species-specific since in human, the interstitial matrix is collagen IV [59]. Since the unidentified cell population on the transition of cortex and medulla was widely spread out over the ovary and did not form distinct structures, we considered them different from corpora albicantia. However, they might have been remnants of corpora albicantia that no longer have any organised structure.

4. Conclusion

For the first time, a description and molecular characterisation, on structures detected in adult white rhinoceros ovaries that deviate from the standard physiological structures, is provided. A combination of histological structure with immunohistochemical characterisation allowed us to verify some differential diagnoses. Deviations from the normal physiology included follicle-like structures (FLS), degenerating, deformed and luteinizing follicles as well as an undefined cell population on the transition of the cortex and medulla. Describing and characterising these aberrant structures, is a crucial step in understanding and explaining ovarian physiology in the southern white rhinoceros. Moreover, knowledge on the ovarian physiology has implications for the development of ART based on the aspiration, dissection or isolation of follicles. Specifically in the context of OPU, FLS might contribute to poor oocyte recovery rates in aged female white rhinoceroses. Their relevance for all rhinoceros species and maybe even other wildlife species in which in vitro embryo production programs have to cope with aged females, remains to be investigated.

CRediT authorship contribution statement

Suzannah A Williams: Writing – review & editing, Writing – original draft, Supervision, Resources, Project administration, Methodology, Investigation, Funding acquisition, Conceptualization. **Thomas B Hildebrandt**: Writing – review & editing, Funding acquisition, Data curation. **Susanne Holtze**: Writing – review & editing, Funding acquisition, Data curation. **Robert Hermes**: Writing – review & editing, Methodology, Investigation, Funding acquisition, Data curation, Conceptualization. **Ruth Appeltant**: Writing – review & editing, Writing – original draft, Project administration, Methodology, Investigation, Funding acquisition, Formal analysis, Data curation, Conceptualization.

Funding

This work was funded by Fondation Hoffmann to S.A.W. supporting R.A., the Covid-19 rebuilding research momentum fund awarded to R.A. (project reference 0009963) and the BMBF project “BioRescue” (01LC1902A) supporting T.B.H. and S.H.

Declaration of Competing Interest

The authors declare the following financial interests/personal relationships which may be considered as potential competing interests: Suzannah Williams reports financial support was provided by Fondation Hoffmann. Thomas Hildebrandt and Susanne Holtze reports financial support was provided by BMBF project BioRescue. Ruth Appeltant reports financial support was provided by Covid-19 rebuilding research momentum fund. If there are other authors, they declare that they have no known competing financial interests or personal relationships that could have appeared to influence the work reported in this paper.

Acknowledgement

The authors would like to acknowledge Dr. Ida Parisi, lab manager of the Histology Facility at the Kennedy Institute of Rheumatology (Oxford) for help with embedding, Dr. Adam Watkins (University of Nottingham), and Dr. Christoffer Lagerholm and Dr Jana Koth, the facility manager of the Wolfson imaging centre Oxford for help with slide scanning. We would also like to acknowledge the input of Prof. N. Smart of the Department of Physiology, Anatomy and Genetics for her insight into blood vessel histology and providing the CD31 antibody. Thanks to the Zoological Society of London (Whipsnade Zoo, UK), the Beekse Bergen (the Netherlands) and Salzburg Zoo (Austria) for providing rhinoceros samples.

Authors' roles

R. Appeltant and S. A. Williams were involved in the conception and design of the study, data interpretation and analysis, and manuscript generation. R. Appeltant carried out data acquisition by generating the data and performing data analysis. R. Hermes, S. Holtze and T. B. Hildebrandt were essential for all aspects of obtaining the rhinoceros samples. R. Hermes, S. Holtze and T. B. Hildebrandt were also involved in data interpretation. All authors contributed to and agreed the final draft of the manuscript.

Appendix A. Supporting information

Supplementary data associated with this article can be found in the online version at doi:10.1016/j.therwi.2024.100096.

References

[1] T.B. Hildebrandt, R. Hermes, F. Goeritz, R. Appeltant, S. Colleoni, B. de Mori, et al., The ART of bringing extinction to a freeze - History and future of species conservation, exemplified by rhinos, Theriogenology 169 (2021) 76–88.
[2] A. Swegen, R. Appeltant, S.A. Williams, Cloning in action: can embryo splitting, induced pluripotency and somatic cell nuclear transfer contribute to endangered species conservation, Biol. Rev. Camb. Philos. Soc. 98 (2023) 1225–1249.
[3] Holt W.V., Brown J.L., Comizzoli P. Reproductive sciences in animal conservation. Adv Exp Med Biol ed. New York: Springer; 2014.
[4] G. Musumeci, Past, present and future: overview on histology and histopathology, J. Histol. Histopathol. 1 (2014).
[5] L.L. de Matos, D.C. Trufelli, M.G.L. de Matos, M.A.S. Pinhal, Immunohistochemistry as an important tool in biomarkers. detection and clinical practice, Biomark. Insights 5 (2010) 9–20.
[6] R. Appeltant, R. Hermes, S. Holtze, S.C. Modina, C. Galli, B.D. Bjarkadottir, et al., The neonatal southern white rhinoceros ovary contains oogonia in germ cell nests, Commun. Biol. 6 (2023) 1049.
[7] R. Hermes, F. Goritz, J. Saragusty, M.A. Stoops, T.B. Hildebrandt, Reproductive tract tumours: the scourge of woman reproduction ails Indian rhinoceroses, PLoS One 9 (2014) e92595.
[8] R. Hermes, F. Schwarzenberger, F. Goritz, S. Oh, T. Fernandes, R. Bernardino, et al., Ovarian down regulation by GnRF vaccination decreases reproductive tract tumour size in female white and greater one-horned rhinoceroses, PLoS One 11 (2016) e0157963.
[9] R. Hermes, T.B. Hildebrandt, C. Walzer, F. Goritz, M.L. Patton, S. Silinski, et al., The effect of long non-reproductive periods on the genital health in captive female white rhinoceroses (Ceratotherium simum simum, C.s. cottoni), Theriogenology 65 (2006) 1492–1515.
[10] N.E. Schaffer, Z. Zainal-Zahari, M.S.M. Suri, M.R. Jainudeen, R.S. Jeyendran, Ultrasonography of the reproductive anatomy in the sumatran rhinoceros (Dicerorhinus sumatrensis), J. Zoo. Wildl. Med. 25 (1994) 337–348.
[11] R.W. Radcliffe, N.M. Czekala, S.A. Osofsky, Combined serial ultrasonography and fecal progestin analysis for reproductive evaluation of the female white rhinoceros (Ceratotherium simum simum): preliminary results, Zoo. Biol. 16 (1997) 445–456.
[12] T.L. Roth, J.K. O'Brien, M.A. McRae, A.C. Bellem, S.J. Romo, J.L. Kroll, et al., Ultrasound and endocrine evaluation of the ovarian cycle and early pregnancy in the Sumatran rhinoceros, Dicerorhinus sumatrensis, Reproduction 121 (2001) 139–149.
[13] S.H. Kim, B.J. Seung, S.H. Cho, H.Y. Lim, M.K. Bae, K.Y. Eo, et al., Ovarian adenocarcinoma with metastases in a white rhinoceros, J. Vet. Diagn. Invest 33 (2021) 366–369.

[14] B.V. Adeniran, B.D. Bjarkadottir, R. Appeltant, S. Lane, S.A. Williams, Improved preservation of ovarian tissue morphology that is compatible with antigen detection using a fixative mixture of formalin and acetic acid, Hum. Reprod. 36 (2021) 1871–1890.
[15] S.A. Williams, P. Stanley, Oocyte-specific deletion of complex and hybrid N-glycans leads to defects in preovulatory follicle and cumulus mass development, Reproduction 137 (2009) 321–331.
[16] R. Appeltant, B.V. Adeniran, S.A. Williams, Fixation in form-acetic allows hyaluronic acid detection in mouse ovaries, Reprod. Fertil. 2 (2021) L10–L12.
[17] A. Salustri, C. Garlanda, E. Hirsch, M. De Acetis, A. Maccagno, B. Bottazzi, et al., PTX3 plays a key role in the organization of the cumulus oophorus extracellular matrix and in in vivo fertilization, Development 131 (2004) 1577–1586.
[18] P. Ploutarchou, P. Melo, A.J. Day, C.M. Milner, S.A. Williams, Molecular analysis of the cumulus matrix: insights from mice with O-glycan-deficient oocytes, Reproduction 149 (2015) 533–543.
[19] S.A. Stubbs, J. Stark, S.M. Dilworth, S. Franks, K. Hardy, Abnormal preantral folliculogenesis in polycystic ovaries is associated with increased granulosa cell division, J. Clin. Endocrinol. Metab. 92 (2007) 4418–4426.
[20] T. Pedersen, H. Peters, Proposal for a classification of oocytes and follicles in the mouse ovary, J. Reprod. Fertil. 17 (1968) 555–557.
[21] B.K.M. Lo, S. Sheikh, S.A. Williams, In vitro and in vivo mouse follicle development in ovaries and reaggregated ovaries, Reproduction 157 (2019) 135–148.
[22] M. Wilson, R. Hermes, J. Bainbridge, H. Bassett, A case of metastatic uterine adenocarcinoma in a southern white rhinoceros (Ceratotherium simum Simum), J. Od. Zoo. Wildl. Med. 41 (2010) 110–113.
[23] S. Nofech-Mozes, N. Ismiil, V. Dube, R.S. Saad, M.A. Khalifa, O. Moshkin, et al., Immunohistochemical characterization of primary and recurrent adult granulosa cell tumors, Int J. Gynecol. Pathol. 31 (2012) 80–90.
[24] S.T. Schumer, S.A. Cannistra, Granulosa cell tumor of the ovary, J. Clin. Oncol. 21 (2003) 1180–1189.
[25] S.S. Guraya, Histophysiology and histochemistry of the interstitial gland tissue in the ovaries of non-pregnant marmosets, Cells Tissues Organs 70 (1968) 623–640.
[26] R. Jimenez, Ovarian organogenesis in mammals: mice cannot tell us everything, Sex. Dev. 3 (2009) 291–301.
[27] Mohammed AHS, T.J. Ali, Z.J. Naki, Histological study of ovarian interstitial glands in IRAQI buffaloes at six and nine years old, J. US-China Med. Sci. 10 (2013) 170–173.
[28] A. Kamnate, J. Sirisin, M. Watanabe, H. Kondo, W. Hipkaeo, S. Chomphoo, Mitochondrial localization of CB1 in progesterone-producing cells of ovarian Interstitial glands of adult mice, J. Histochem Cytochem 70 (2022) 251–257.
[29] P. Bagavandoss, S. Grimshaw, Temporal and spatial distribution of the cannabinoid receptors (CB1, CB2) and fatty acid amide hydroxylase in the rat ovary, Anat. Rec. (Hoboken) 293 (2010) 1425–1432.
[30] N. Battista, M. Bari, M. Maccarrone, Endocannabinoids, Springer, 2015.
[31] G. Galiazzo, F. Giancola, A. Stanzani, F. Fracassi, C. Bernardini, M. Forni, et al., Localization of cannabinoid receptors CB1, CB2, GPR55, and PPARalpha in the canine gastrointestinal tract, Histochem Cell Biol. 150 (2018) 187–205.
[32] A. Kulkarni-Narla, D.R. Brown, Localization of CB1-cannabinoid receptor immunoreactivity in the porcine enteric nervous system, Cell Tissue Res 302 (2000) 73–80.
[33] Y. Knauf, K. Kohler, S. Knauf, A. Wehrend, Histological classification of canine ovarian cyst types with reference to medical history, J. Vet. Sci. 19 (2018) 725–734.
[34] H.A. Garverick, Ovarian follicular cysts in dairy cows, J. Dairy Sci. 80 (1997) 995–1004.
[35] R. Hermes, F. Goritz, T.J. Portas, B.R. Bryant, J.M. Kelly, L.J. Maclellan, et al., Ovarian superstimulation, transrectal ultrasound-guided oocyte recovery, and IVF in rhinoceros, Theriogenology 72 (2009) 959–968.
[36] R.J. Rodgers, H.F. Irving-Rodgers, Formation of the ovarian follicular antrum and follicular fluid, Biol. Reprod. 82 (2010) 1021–1029.
[37] K.J. Hutt, E.A. McLaughlin, M.K. Holland, Primordial follicle activation and follicular development in the juvenile rabbit ovary, Cell Tissue Res 326 (2006) 809–822.
[38] I.L. van Wezel, H.F. Irving-Rodgers, Y. Sado, Y. Ninomiya, R.J. Rodgers, Ultrastructure and composition of call-exner bodies in bovine follicles, Cell Tissue Res 296 (1999) 385–394.
[39] T.B. Hildebrandt, S. Holtze, S. Colleoni, R. Hermes, J. Stejskal, I. Lekolool, et al., In vitro fertilization program in white rhinoceros, Reproduction 166 (2023) 383–399.
[40] T.B. Hildebrandt, R. Hermes, S. Colleoni, S. Diecke, S. Holtze, M.B. Renfree, et al., Embryos and embryonic stem cells from the white rhinoceros, Nat. Commun. 9 (2018) 2589.
[41] M. Papas, J. Govaere, S. Peere, I. Gerits, M. Van de Velde, D. Angel-Velez, et al., Anti-mullerian hormone and OPU-ICSI outcome in the mare, Animals 11 (2021).
[42] A. Claes, T.A.E. Stout, Success rate in a clinical equine in vitro embryo production program, Theriogenology 187 (2022) 215–218.
[43] S.-S. Kang, U.-H. Kim, S.-D. Lee, M.-S. Lee, M.-H. Han, S.-R. Cho, Recovery efficiency of cumulus oocyte complexes (COCs) according to collection frequency for ovum pick-up (OPU) method in hanwoo cow, J. Anim. Reprod. Biotechnol. 34 (2019) 300–304.
[44] J.S. Merton, A.P.W. de Roos, E. Mullaart, L. de Ruigh, L. Kaal, P.L.A.M. Vos, et al., Factors affecting oocyte quality and quantity in commercial application of embryo technologies in the cattle breeding industry, Theriogenology 59 (2003) 651–674.
[45] I. Brunel, S. Iacoponi, A. Hernandez, M.D. Diestro, J. De Santiago, I. Zapardiel, Intravascular leiomyomatosis: an exceptional entity, Clin. Exp. Obstet. Gynecol. 43 (2016) 443–445.
[46] R. Hermes, T.B. Hildebrandt, F. Goritz, Reproductive problems directly attributable to long-term captivity–asymmetric reproductive aging, Anim. Reprod. Sci. 82-83 (2004) 49–60.
[47] E.M. Yousef, D. Furrer, D.L. Laperriere, M.R. Tahir, S. Mader, C. Diorio, et al., MCM2: An alternative to Ki-67 for measuring breast cancer cell proliferation, Mod. Pathol. 30 (2017) 682–697.
[48] C.R. Harlow, L. Davidson, K.H. Burns, C. Yan, M.M. Matzuk, S.G. Hillier, FSH and TGF-beta superfamily members regulate granulosa cell connective tissue growth factor gene expression in vitro and in vivo, Endocrinology 143 (2002) 3316–3325.
[49] M. Mattioli, A. Gloria, M. Turriani, P. Berardinelli, V. Russo, D. Nardinocchi, et al., Osteo-regenerative potential of ovarian granulosa cells: an in vitro and in vivo study, Theriogenology 77 (2012) 1425–1437.
[50] N.A. Johnson, M. Boyle, A. Bashashati, S. Leach, A. Brooks-Wilson, L.H. Sehn, et al., Diffuse large B-cell lymphoma: reduced CD20 expression is associated with an inferior survival, Blood 113 (2009) 3773–3780.
[51] S.M. Briley, S. Jasti, J.M. McCracken, J.E. Hornick, B. Fegley, M.T. Pritchard, et al., Reproductive age-associated fibrosis in the stroma of the mammalian ovary, Reproduction 152 (2016) 245–260.
[52] R. van de Lagemaat, C.J. van Koppen, M.A. Krajnc-Franken, B.J. Folmer, H.A. van Diepen, S.M. Mulders, et al., Contraception by induction of luteinized unruptured follicles with short-acting low molecular weight FSH receptor agonists in female animal models, Reproduction 142 (2011) 893–905.
[53] S.A. Williams, P. Stanley, Premature ovarian failure in mice with oocytes lacking core 1-derived O-glycans and complex N-glycans, Endocrinology 152 (2011) 1057–1066.
[54] N. Mimoune, M.H. Benaissa, R. Baazizi, S. Radhwane, A.M. Yassine, B. Ayed, et al., Histological and immune-histochemical evaluation of ovarian cysts in cattle, Rumin. Sci. 9 (2020) 1–6.
[55] N.R. Salvetti, M.L. Stangaferro, M.M. Palomar, N.S. Alfaro, F. Rey, E.J. Gimeno, et al., Cell proliferation and survival mechanisms underlying the abnormal persistence of follicular cysts in bovines with cystic ovarian disease induced by ACTH, Anim. Reprod. Sci. 122 (2010) 98–110.
[56] C. Stanley, S.E. O'Sullivan, Vascular targets for cannabinoids: animal and human studies, Br. J. Pharm. 171 (2014) 1361–1378.
[57] G.R.D.A. Focchi, M.D.J. Simoes, E.C. Baracat, G.R.D. Lima, J.E. Neto, Ultrastructural aspects of the remodeling process of the Corpus albicans in the recent postmenopausal period, Sao Paulo Med. J. 114 (1996) 1173–1176.
[58] M.R. Luck, Y. Zhao, L.M. Silvester, Identification and localization of collagen types I and IV in the ruminant follicle and corpus luteum, J. Reprod. Fertil. Suppl. 49 (1995) 517–521.
[59] H.F. Irving-Rodgers, B.E. Friden, S.E. Morris, H.D. Mason, M. Brannstrom, K. Sekiguchi, et al., Extracellular matrix of the human cyclic corpus luteum, Mol. Hum. Reprod. 12 (2006) 525–534.